Phenylpropenoids from *Bupleurum fruticosum* as Anti-human Rhinovirus Species A Selective Capsid Binders

Benedetta Fois,[†,▽] Giulia Bianco,[†,▽] Vijay P. Sonar,[†] Simona Distinto,[†] Elias Maccioni,[†] Rita Meleddu,[†] Claudia Melis,[†] Luisa Marras,[‡] Raffaello Pompei,[‡] Costantino Floris,[§] Pierluigi Caboni,[†] and Filippo Cottiglia[*,†]

[†]Department of Life and Environmental Sciences, University of Cagliari, via Ospedale 72, 09124 Cagliari, Italy

[‡]Department of Biomedical Sciences, University of Cagliari, Cagliari, Italy

[§]Dipartimento di Scienze Chimiche, University of Cagliari, Cittadella di Monserrato, 09042, Monserrato, Cagliari, Italy

ABSTRACT

The dichloromethane extract of the leaves of *Bupleurum fruticosum* was found to inhibit the replication of human rhinovirus (HRV) serotypes 14 and 39. Bioassay-guided fractionation led to the isolation of seven phenylpropenol derivatives (**3**-**9**), two polyacetylenes (**1**-**2**) and one monoterpene (**10**). Compounds **1** and **10** were identified as previously undescribed secondary metabolites after extensive 1D and 2D NMR experiments as well as high resolution mass spectrometry. Compounds **2**, **4** and **5** showed a selective inhibition of viral replication against HRV 39 serotype with **2** and **4** being the most active with EC_{50} values of 1.8 ± 0.02 μM and 2.4 ± 0.04 μM. Mechanism of action studies indicated that **4** behaves not only as a capsid binder, interfering with the early phases of virus replication, but also as a late-phase replication inhibitor. Docking experiments were performed to confirm the ability of the antiviral phenylpropenoids to selectively fit into the hydrophobic pocket of VP1-HRV39.

Human rhinovirus (HRV) is the leading cause of mild upper respiratory illness and is considered to be among the most frequent infectious agents in humans worldwide.[1] Although HRV infections are often mild and self-limiting they lead to economic burdens in terms of medical visits and school and work absenteeism.[1] Furthermore, HRV is also responsible of viral induced asthma exacerbations and chronic obstructive pulmonary disease (COPD) in children and adults as well as fatal pneumonia in immunocompromised adults.[1] COPD is predicted by the World Health Organization to become the third leading cause of death worldwide by the year 2030.[2] Despite the fact that many small molecules have been identified as rhinovirus inhibitors, none has been approved as an antiviral drug so far. Nevertheless, various compounds have been submitted to clinical trials and some of them are still under evaluation by U.S. FDA. Among all, pleconaril is one of the most promising antirhinovirus drugs, and it exhibit good efficacy against many HRV serotypes in phase III clinical trials. However, due to the occurrence of drug-drug interactions and the emerging of drug resistance, FDA did not approve the oral administration of pleconaril for the treatment of common cold.[3] However, a phase II trial to evaluate the efficacy of a spray intranasal formulation of pleconaril in preventing asthma exacerbation and common cold symptoms in asthmatic participants was concluded in 2007. The results have not been published until recently.[4] Pirodavir, a pyridazine analogue of pleconaril, is able to inhibit the replication of HRV at nanomolar concentrations but no clinical efficacy was found due to its poor pharmacokinetic properties.[5] More recently, another molecule named vapendavir, showed high efficacy for the treatment/prevention of rhinovirus-induced exacerbations of asthma with favorable pharmacokinetic and toxicological profiles.[6] All these compounds are known as "capsid binders", because they are able to interact with capsid proteins. In particular, a large cleft (''canyon'') is present on each icosahedral face of the virus and capsid binders are able to fit into

the hydrophobic pocket, underneath the canyon floor. The formation of such a complex induces conformational changes of the HRV canyon, hinders virus-receptor interactions, and prevents attachment to host cells and/or virus uncoating.[7] Various plant extracts, such as from *Panax quinquefolium*, *Pelargonium sidoides*, *Allium*, *Echinacea*[7] and *Bupleurum* species[8] have been used in the traditional medicine to treat or prevent common cold. *Bupleurum fruticosum* L. (Apiaceae) is a shrub distributed in the southern Mediterranean area and particularly in Sardinia. The traditional medicinal uses of *B. fruticosum* has been known for millenia. Dioscorides indicated this plant to be an emmenagogue and useful for treating strangury, urethral straggling, orthopnoea and epilepsy.[9] In Sardinia, *B. fruticosum* has been used in folk medicine as an antirheumatic remedy.[10] Previous phytochemical studies on the leaves of *B. fruticosum* revealed as main secondary metabolites phenylpropanoids with anti-inflammatory activity,[10-12] triterpenoid saponins[13] and coumarins.[13]

As part of a continuing research aimed at the discovery of antiviral compounds from higher plants,[14] the CH_2Cl_2 extract of the leaves of *Bupleurum fruticosum* was studied based on the antiviral activity against HRV14 and HRV39.The two serotypes differ from each other in amino acid composition, the shape of the capsid proteins and in the size of the ligand-binding site within the VP1 capsid protein. The CH_2Cl_2 extract of *B. fruticosum* inhibited the replication of HRV 39 and HRV 14 with EC_{50} values of 3.1 ± 0.5 and 12.5 ± 0.8 μg/mL, respectively, with low cytotoxicity against HeLa cells (CC_{50} 125 ± 31 μg/mL) (Table S1, Supporting Information). Thus, this CH_2Cl_2 extract was subjected to a bioguided-fractionation in order to purify the bioactive compound(s).

RESULTS AND DISCUSSION

The plant CH_2Cl_2 extract was subjected to fractionation by silica gel vacuum-liquid chromatography (VLC) obtaining six major fractions (F1-F6). Each fraction was then tested against HRV39 and HRV14. Among all, only F3 was able to inhibit the replication of both rhinovirus forms with an EC_{50} of 6.2 ± 0.6 μg/mL. Furthermore, F3 exhibited low cytotoxicity towards HeLa cells (CC_{50} 62 ± 5 μg/mL) and a Selective Index (SI: CC_{50}/EC_{50}) of 10 (Table S1, Supporting Information). Pleconaril, a selective capsid binder, was used as reference compound. F3 was purified by column chromatography (silica gel and Sephadex LH 20) and semi-preparative NP (normal-phase) or RP (reversed-phase) HPLC to give one polyacetylene (**2**), three phenylpropenoids (**4**, **5**, **8**) and one monoterpene (**10**). With the aim to developing preliminary structure-activity relationship information, the chemical composition of fractions F1, F2 and F4 were investigated, yielding another polyacetylene (**1**) and further four phenylpropenoids (**3**, **6**, **7**, **9**). Compounds **1** and **10** are previously undescribed secondary metabolites.

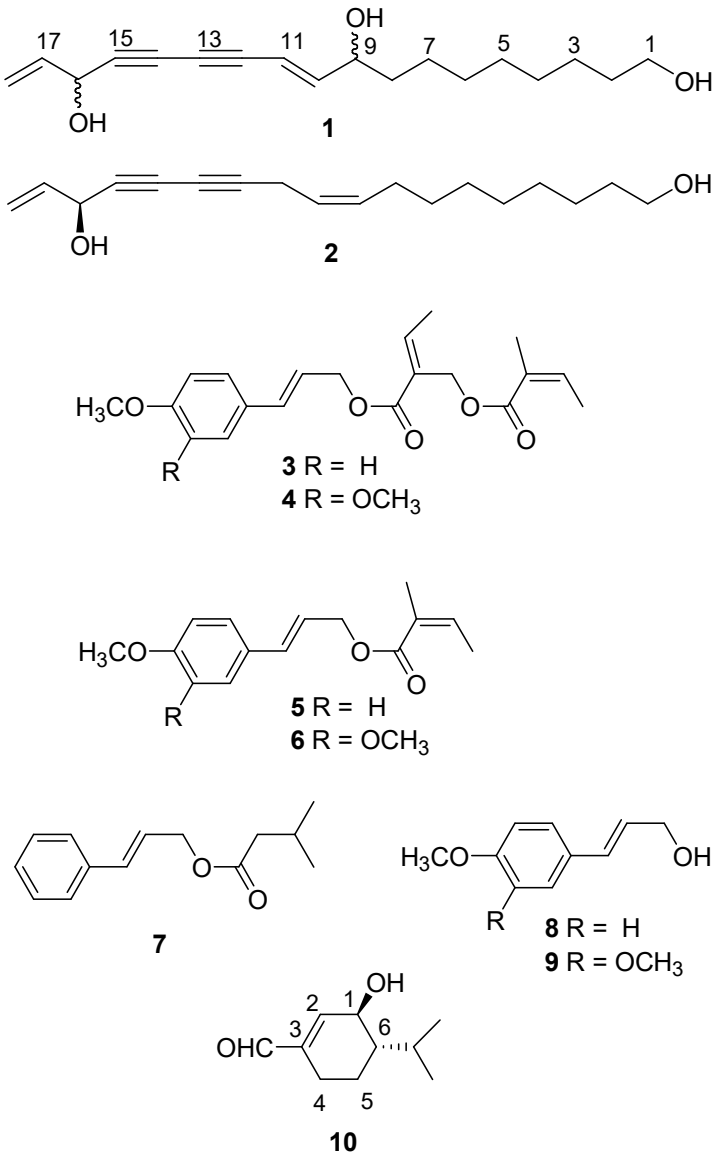

Compound **1** showed an ion peak at *m/z* 289.1802 $[M - H]^-$ (calcd 289.1803) in the HRTOFESIMS, accounting for an elemental composition of $C_{18}H_{26}O_3$. The ^1H NMR spectrum of compound **1** revealed five olefinic proton signals at δ 6.33 (1H, dd, *J* = 5.5, 16 Hz), 5.96 (1H, ddd, *J* = 17.5, 10.0, 5.0 Hz), 5.78 (1H, d, *J* = 16 Hz), 5.48 (1H, d, *J* = 17.5 Hz) and 5.26 (1H, d, *J* = 10.0 Hz), two oxygenated methine proton signals at δ 4.97 (1H, d, *J* = 5.0 Hz) and 4.19 (1H, dt, *J* = 6.5 Hz), one oxymethylene group at δ 3.64 (2H, t, *J* = 7.0 Hz) and two cluster of

methylene proton signals at δ 1.54 (m) and 1.30 (m) (Table 1). Analysis of the ^{13}C NMR spectrum showed 18 signals, of which four quaternary carbons at δ 80.6, 77.4, 73.6 and 70.7 were characteristic of a diyne (Table 1). The HSQC experiments permitted the assignment of each proton to the corresponding carbon. In turn, the ^{1}H-^{1}H COSY spectrum showed correlations between the vinyl proton at 5.96 ppm and the oxymethine at 4.97 ppm and the terminal methylene protons at 5.48 and 5.26 ppm that, besides the cross-peaks observed in the HMBC spectrum between the methylene protons at δ 5.48 and 5.26 and the carbons at 136.0 and 63.48 ppm and between the oxymethine at 4.97 ppm and the carbons at 136.0, 117.0, 80.6, 70.7 and 73.6 ppm, permitted the partial structure CH_2=CH-CH(OH)-C≡C-C≡C- to be established (Figure 1). Further HMBC correlations observed from the proton at δ 5.78 to 77.4, 73.6, 149.9 and 71.9 ppm, and from the oxymethine at δ 4.19 to 149.9, 108.0, 36.7 and 25.1 ppm, were used to locate the olefinic protons occurring at 6.33 and 5.78 ppm to C-10 and C-11, respectively, and the secondary alcoholic group resonating at 4.19 ppm, at C-9 (Figure 1). The geometry at the double bond at C-10 was clearly *trans* according to the coupling constant between H-10 and H-11 ($J_{10,11}$ = 16 Hz). In the ^{1}H NMR spectrum of compound **1**, the absence of a methyl group and the cross-peaks observed in the HMBC spectrum between the oxymethylene protons at δ 3.64 (δ_C 62.9) and C-2 (δ_C 32.6) and C-3 (δ_C 25.6) were used to place the primary alcohol at C-1. The absolute configuration of **1** could not be determined by NMR experiments. An attempt to assign the configuration at C-9 and C-16 by the Mosher ester method failed because of the instability of the molecule. Thus, the structure of **1** was established as *trans*-10,17-octadecadien-12,14-diyne-1,9,16-triol, and was named fruticotriol.

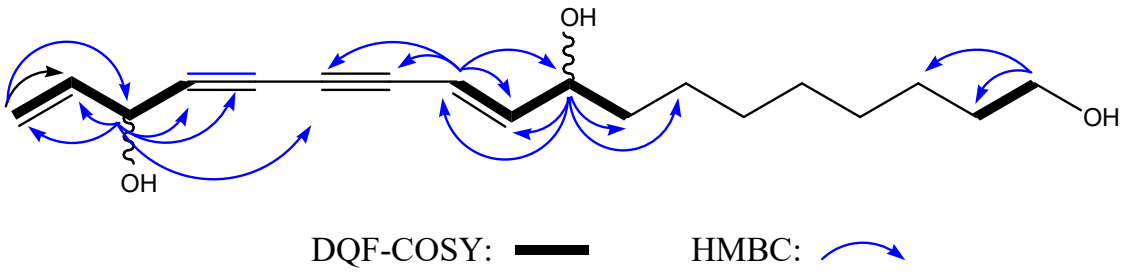

Figure 1. Main HMBC and DQF-COSY correlations of compound **1**

The ^{1}H- and ^{13}C NMR data (Table 1) as well as the 2D NMR experiments (^{1}H-^{1}H COSY, HSQC and HMBC) of compound **10** were in agreement with the structure of eucamalol.[16] The $J_{1,6}$ value (9 Hz) between the protons at δ 4.27 (H-1) and δ 1.38 (H-6) of compound **10** showed an axial-axial coupling suggesting a *trans* disposition of the hydroxy and isopropyl groups. As a consequence, two stereoisomers were congruent with the experimental data. Satoh et al.[17] reported for the synthesized (+)-eucamalol, possessing a *trans* disposition, an absolute configuration 1*R*, 6*R* with a specific optical rotation $[\alpha]^{25}_{D}$ + 14.1 whereas its epimer, (-)-1-*epi*-eucamalol, showed a specific rotation of -234.6. Since for compound **10** a *trans* disposition has found for H-1 and H-6 and an optical rotation of -17.0 measured, compared with (+)-eucamalol, it must have an absolute configuration 1*S*, 6*S* and thus compound **10** was assigned 1*S*,6*S*-(-)-3-formyl-6-isopropyl-2-cyclohexen-1-ol. Therefore, compound **10** is a previously undescribed natural compound and which was named (-)-eucamalol.

The spectroscopic (^{1}H- and ^{13}C-NMR, UV and MS) and physical data (melting point, optical rotation) of the known compounds *cis*-9,17-octadecadiene-12,14-diyne-1,16-diol (**2**),[18] (E)-3-(4-methoxyphenyl)-2-propen-1-yl (Z)-2-[(Z)-2-methyl-2-butenoyloxymethyl)butenoate (**3**),[11] (E)-3-

(3,4-dimethoxyphenyl)-2-propen-1-yl (Z)-2-[(Z)-2-methyl-2-butenoyloxymethyl)butenoate (**4**),[11] 4-*O*-methylcinnamyl angelic acid ester (**5**),[19] 4-*O*-methyl-(*E*)-coniferyl angelic acid ester (**6**),[19] cinnamyl isovalerate (**7**),[20] 4-methoxycinnamyl alcohol (**8**)[21] and 3,4-dimethoxycinnamyl alcohol (**9**)[22] were in agreement with the literature data.

Table 1. ^{1}H NMR and ^{13}C NMR Spectroscopic Data for Compounds **1** and **10** ($CDCl_3$, δ in ppm)

	compound **1**		compound **10**	
position	δ_C, type	δ_H (*J* in Hz)	δ_C	δ_H (*J* in Hz)
1	62.9, CH_2	3.64, t (7.0)	69.3, CH	4.30, dd (9.0, 2.5)
2	32.6, CH_2	1.55, m	151.3, CH	6.64, brs
3	25.6, CH_2	1.29, m[c]	141.9, C	
4	29.4, CH_2[a]	1.29, m[b]	21.6, CH_2	2.39, dd (18, 2.5) 2.03 m
5	29.3, CH_2[a]	1.29, m[b]	20.2, CH_2	1.81 ddt, (13.5, 5.2, 3.0) 1.28, ddt (13.5, 12.0, 5.5)
6	29.1, CH_2	1.29, m[b]	47.8, CH	1.41, ddt (12.0, 9.5, 3.0)
7	25.1, CH_2	1.29, m[b]	193.9, CH	9.50, s
8	36.7, CH_2	1.54, m	26.7, CH	2.09, m
9	71.9, CH	4.19, dt (6.5)	20.9, CH_3	1.01, d (7.0)
10	149.9, CH	6.33, dd, (5.5, 16)	16.4, CH_3	0.88, d (7.0)
11	108.0, CH	5.78, d, (16)		
12	77.4, C			
13	73.6, C			
14	70.7, C			
15	80.6, C			
16	63.5, CH	4.97, d, (5.0)		

17	136.0, CH	5.96, ddd, (17.5, 10.0, 5.0)
18	117.0, CH_2	Ha: 5.48, brd, (17.5) Hb: 5.26, brd, (10.0)

[a]Exchangeable. [b]Signals were overlapped.

The cytotoxicity against HeLa cells and the antirhinovirus (HRV39 and HRV14) activities of the isolated compounds are reported in Table 2. Among the phenylpropenoids, the most active was compound **4** with a EC_{50} value of 2.4 ± 0.04 μM against HRV 39 and moderate cytotoxicity versus HeLa cells (20.3 ± 1.8 μM). The SI was 8.4. For compound **4**, the substitution of a methoxy group at C-3 position of the phenyl ring with a hydrogen, as in compound **3**, annulled the activity (EC_{50} > 36.3 μM) and increased the cytotoxicity. The replacement at the same time of the angeloyl and 3-methoxy groups with a hydrogen atom, as in compound **5**, led to a reduced activity (~ 10 fold). An ester functionality seems essential for the antiviral activity since compounds **8** and **9** proved to be completely inactive. A 3,4-dimethoxyphenyl ring and an ester function was necessary but not sufficient since **6**, containing a shorter alkyl chain with respect to **4**, was not able to inhibit the replication of HRV_S. The polyacetylene **2** was the most active inhibitor of HRV39 replication with a EC_{50} of 1.8 ± 0.02 μM but the cytotoxicity was higher (14.6 ± 0.7 μM) with respect to **4**, although the SI was comparable. The new polyacetylene **1** was not able to inhibit the replication of both HRV serotypes probably due to a greater hydrophilicity and/or to the different double bond geometry when compared to compound **2**. Interestingly, the compounds are able to inhibit only HRV39 indicating a selective action towards the group A species.

Table 2**.** Cytotoxic and Antirhinovirus Activities of Compounds **1-10**

compound	CC_{50}[a] µM	EC_{50}[b] µM	EC_{50}[b] µM (SI[c])
	HeLa	HRV14	HRV39
1	107 ± 0.75	>107	>107
2	14.6 ± 0.7	>14.6	1.8 ± 0.02 (8.1)
3	36.3 ± 2.1	>36.3	>36.3
4	20.3 ± 1.8	>20.3	2.4 ± 0.04 (8.4)
5	248 ± 1.5	>248	30.9 ± 0.9 (8)
6	453 ± 31	>453	>453
7	142 ± 1.5	>142	>142
8	189 ± 2.5	>189	>189
9	160 ± 2.2	>160	>160
10	47.6 ± 0.7	>47.6	>47.6
pleconaril	131 ± 1.2	0.3 ± 0.01	0.1 ± 0.01

[a]CC_{50}: cytotoxic concentration for 50% of cell death, measured with MTT assay in HeLa cells; [b]EC_{50}: Effective concentration for 50% inhibition of each HRV species measured with MTT assay in HeLa cells; [c]SI: Selective index, calculated by CC_{50}/EC_{50}

A series of compounds designed by a structure-based approach, able to inhibit the replication of HRV14 (rhinovirus B), but not HRV2 (rhinovirus A), has been recently reported.[23,24] Molecular modeling studies also demonstrated that these compounds were able to bind into the pocket the canyon of the HRV14 VP1 protein. Compound **4**, a highly lipophilic compound, showed similarity with the above-mentioned synthesized compounds but, interestingly, this 3,4-dimethoxybenzene derivative was selective toward group A serotypes with no activity towards group B. These differences could be explained by a diverse amino acid composition and shape of

the two rhinovirus groups. Compound **3**, not active in the present assay, was selected by Rollinger et al.[25] as a virtual HRV16 (rhinovirus A) capsid binder hit from a natural 3D database. On the basis of these findings, it can be assumed that also compounds **4** and **5** could be HRV capsid binders.

In order to elucidate the mechanism of action of the most active and stable compound, its antiviral activity on the inhibition of HRV39 replication in a time-of-drug addition assay was evaluated. Despite its interesting activity, compound **2** was not tested due to its chemical instability. Figure 2 shows the effects of varying the time of addition of compound **4** (5 μg/mL) on the inhibition of HRV 39 replication. The antiviral activity of compound **4** was assessed in a multi-cycle, virus-cell-based cytopathic effect (CPE) reduction assay in HeLa cells. Pirodavir (5 μg/mL) was used as reference compound. The treatment of cells with compound **4** prior to infection reduced by 100% the virus yield, suggesting an ability of this substance to adsorb to the cell surface in a suitable position to prevent infection. Almost the same level of inhibition (90%) was observed when **4** was added to cells together with the virus and maintained until the end of HRV39 multiplication. This behavior was similar to that expressed by pirodavir, and showed that **4** is an antiviral agent that exerts its activity in the early phases of viral replication and behaves as a capsid binder towards HRV 39. In contrast to pirodavir, addition of **4** to infected HeLa cells 1 h after post binding still resulted in a strong reduction in virus yield (78%). Addition of **4** to the infected culture medium after 2-3 h post binding was less effective (65% and 50% reduction, respectively), but still significant. The considerable inhibitory effect of compound **4** when added after virus binding (1-3 h) strongly suggested the capability of this substance to enter the host cells and to act with a further mode of action probably based on the uncoating of viral genome or on inhibition of protein synthesis.

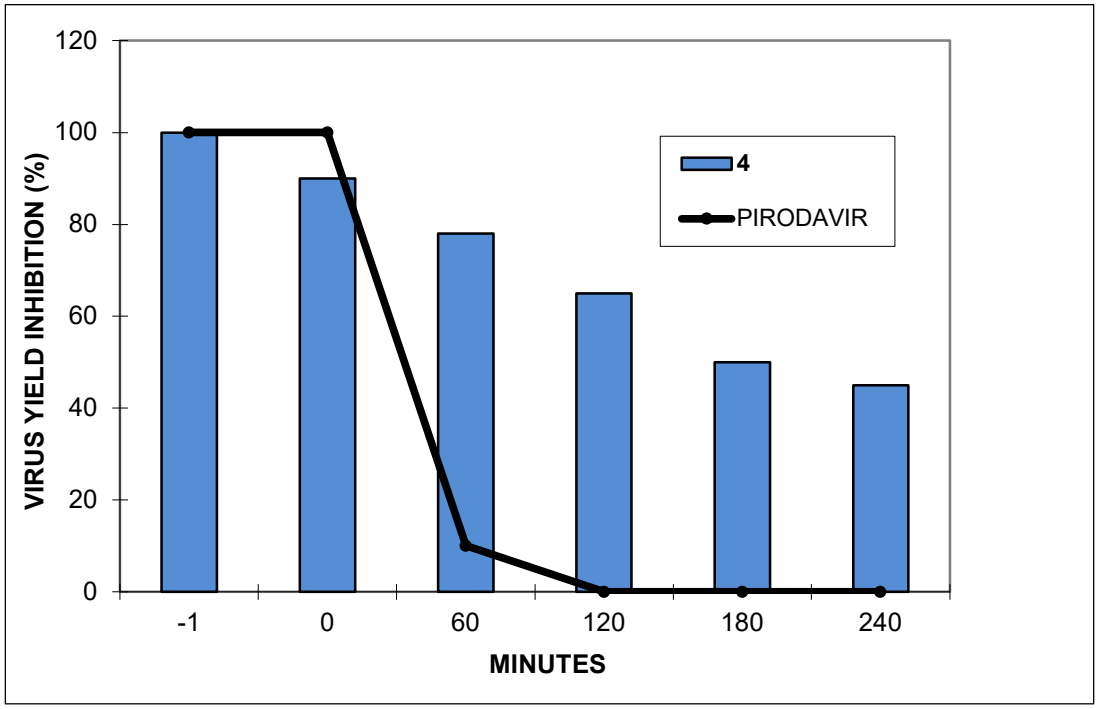

Figure 2. Effect of addition of **4** and pirodavir at different times during the HRV growth cycle in HeLa cells. Compound **4** and pirodavir were both used at a concentration of 5 µg/mL. Compounds were added prior to (-1 h), at the time of (0 h), or after viral infection (1-4 h) at the indicated time points and virus yield inhibition (%) was determined by a virus-cell-based cytopathic effect (CPE) reduction assay in HeLa cells.

In the light of the experimental results exhibited by the isolated compounds, computational studies were carried out in order to identify the key residues involved in the interaction with the enzyme. Since no crystal structure of the coat protein-VP1 HRV39 is available in the Protein Data Bank (PDB), the structure was built with Swiss model,[26] a fully automated protein structure homology-modelling server. The sequence of coat protein VP1 of HRV39 was retrieved from the Uniprot server (Uniprot code: Q7T625; Figure S7, Supporting Information). This sequence was

fed into the BLAST search tool. BLAST was able to identify two sequences: VP1 of HRVA1 (i.e., sequence 1R1A, 2HWD, 2HWE, 2HWF; named Group 1) with 76% sequence identity and VP1 of HRV16 (1AYM, 1AYN, 1QJU, 1QYX, 1QJY, 1C8M, 1NCR, 1ND2, 1ND3; Group 2) that share a 74% of identity with the target structure. Two representative structures of Group 1 and 2 were aligned in order to analyze the binding pocket and the residues around 4 Å of the co-crystallized ligand were compared with the residues of VP1-HRV39 through the multiple alignment with Clustal Omega.[27] This analysis highlighted that the binding pocket of HRV16-VP1 (1AYM) is more similar to VP1-HRV39 than HRVA1-VP1 (1R1A) (Figure S8, Supporting Information). Hence the 1AYM[28] crystal structure was used as a template, although no co-crystalized ligand was accommodated inside the binding pocket. In fact, this crystal structure showed the best resolution (2.15 Å) among the other complexes of Group 2. Indeed, the alignment of the unbound crystal with the complexes of VP1-HRV16 did not reveal any relevant difference with the apoenzyme. The same observation was reported for VP1 of HRVA1, while in contrast VP1 of HRV14 goes through consistent conformational change upon ligand binding.[29] The quality of the homology model was assessed by Swiss Model through the measure of qmean[30] and through comparison with non-redundant PDB structures (Figure S9, Supporting Information). subsequently, by ERRAT (Figure S10, Supporting Information)[30] and PROCHECK (Figure S11, Supporting Information).[31] Therefore, this protein was considered as a reliable model for the molecular docking of unknown compounds. Since no complexes of VP1-HRV39 are available, the docking experiment protocol initially was validated by performing cross-docking experiment by taking into account the VP1 complexes of HRV16, since the two proteins are very similar. In particular, the compounds WIN61209 (W01), WIN6934 (W02), WIN65099 (W03) and pleconaril (WIN63843) were docked inside the crystal structure that was

used as a template for homology modeling (1AYM). The best results were obtained with the Quantum-mechanics Polarized Docking protocol (QMPL) (Figure S12, Table S2, Supporting Information).[32,33] This protocol was then applied to analyze the putative binding mode of the phenylpropenoids **4** and **5** into the validated model of the VP1-HRV39 structure. These two compounds appeared as the most interesting since they showed the lowest EC_{50} values against VP1-HRV39. The best three scored poses of each docked ligand were subjected to a post-docking protocol based on energy minimization and binding-free energy calculation applying molecular mechanics and continuum solvation models using the molecular mechanics generalized Born/surface area method (MM-GBSA)[34] in order to take into account induced fit phenomena, which occurs after ligand binding (Figure 3). In parallel with this procedure, the same protocol was used to dock the new compounds inside the crystal structure of VP1 HRV14, having the code 1NCQ, which is the crystal structure with the best resolution (2.5 Å) among the structures retrieved from the Protein Data Bank (Figure S12, Supporting Information).[35] After a detailed visual inspection, identification of the key residues involved in the interaction of VP1-HRV39 with the unknown compounds was carried out. The binding pocket is characterized by the presence of highly hydrophobic residues. Some of these residues are the same as recognized by a previous pharmacophore-based virtual screening_ENREF_7 of compounds targeting VP1-HRV16 as hydrophobic features of the pharmacophore.[25] In particular, the conserved residues are Tyr145, Leu101, Ile123, Tyr191 and Leu185, while Ile237 is substituted by a valine in VP1-HRV39. In addition to these important interactions, complexes of compounds **4** and **5** were stabilized by hydrogen bonds with Thr100 and Asn213, with the oxygen of the methoxy group of the phenyl ring, respectively (Figure 3).

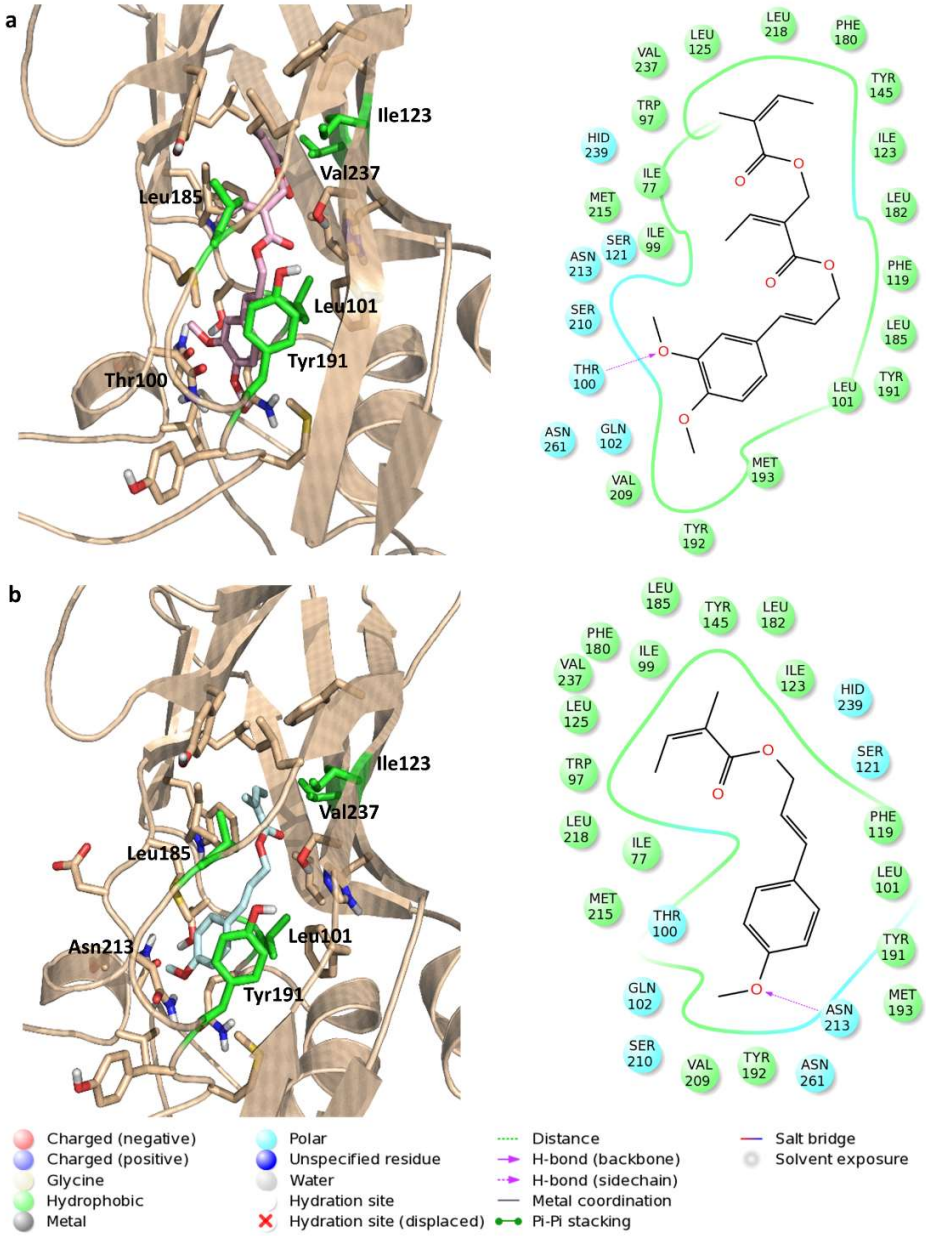

Figure 3. 3D and relative 2D representation of (a) compound **4** (pink) and (b) compound **5** (light blue) putative binding mode resulting from the docking experiments into the built model of VP1-HRV39. The key residues are highlighted in green in the 3D depiction.

Both compounds **4** and **5** are able to occupy most of the binding site of VP1-HRV39 but the major activity of **4** could be explained through the analysis of the number of interactions and through the measure of the free energy of interaction performed with the post-docking procedure. In fact, compound **4** is able to deeply occupy the hydrophobic pocket of the protein and showed a lower value of total energy of interaction (-50.74 kcal/mol, Table S3, Supporting Information) indicating a major stability of the complex. Compound **5** showed a higher value (-42.54 kcal/mol, Table S3, Supporting Information). This fact can be also explained through the analysis of the chemical characteristics of the compounds and the binding site. In fact, the VP1-HRV39 pocket is highly hydrophobic as seen with the software SiteMap[36] that generate maps within the binding site suitable for occupancy by ligand hydrophobic hydrogen-bond donor, acceptor groups. Compound **4** was well accommodated (Figure 4) and fit nicely the binding pocket. Furthermore, analysis of the maps gave also information about possible modifications that could lead to compound optimization.

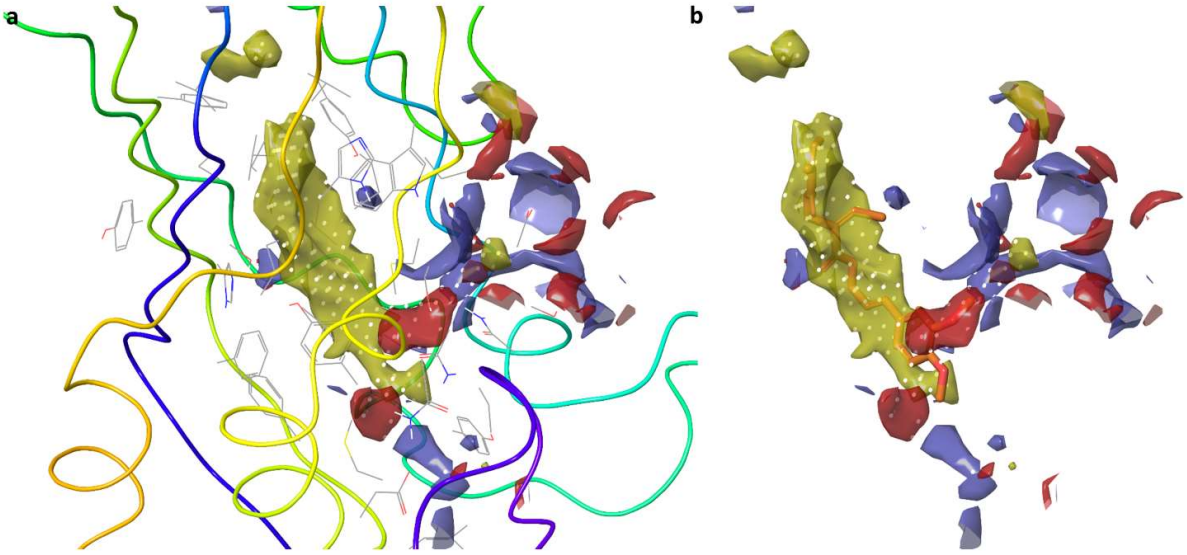

Figure 4. Sitemap visualization of active site maps: (a) Regions within the binding site suitable for occupancy by hydrophobic groups (yellow) or by ligand hydrogen-bond donors (blue), acceptors (red) of VP1-HRV39; (b) Superimposition of compound **4** docking pose (in orange) and Sitemap highlighted regions.

The analyzed compounds **4** and **5** showed a good inhibitory activity towards HRV39 while the lower efficacy towards HRV14 could be explained by the differently interactions of these compounds with VP1. In fact, inside 1NCQ (HRV14) both compounds interact with different residues because the presence of Tyr128 with its steric hindrance does not allow a proper accommodation into the hydrophobic binding pocket (Figure S13, Supporting Information). In VP1-HRV39, this tyrosine is replaced by an isoleucine, which is a key residue in protein-compound interaction. Furthermore, the lowest activity is well explained by the post-docking results that showed higher values of total energy of interaction for VP1-HRV14 with respect to VP1-HRV39 (Table S3, Supporting Information).

In summary, by means of bioguided-isolation three compounds (**2**, **4**-**5**) were found responsible for the antirhinovirus activity of the dichloromethane extract of *B. fruticosum*. Among all, the polyacetylene *cis*-9,17-octadecadiene-12,14-diyne-1,16-diol (**2**), even if the most active, was unstable both in polar and apolar solvents. This fact, together with its skin sensitizer action,[37] due to the conjugated triple bonds,[38] would prevent any therapeutic utilization against the common cold. In contrast, the phenylpropene **4**, almost as potent as **2**, was stable and behaved as an antirhinovirus species A selective capsid binder. Furthermore, a time-of-drug addition assay highlighted the potential of a multi-target action for this compound, which should enhance

interest in the development and the optimization of new synthetic analogues with better selectivity indices and/or potencies.

EXPERIMENTAL SECTION

General Experimental Procedures. All melting points were determined on a Köfler apparatus and are uncorrected. Optical rotations were measured in $CHCl_3$ or MeOH at 25 °C using a Perkin-Elmer 241 polarimeter. UV spectra were recorded on a GBC Cintra 5 spectrophotometer. NMR spectra of all isolated compounds were recorded at 25 °C on Unity Inova 500NB high-resolution spectrometer (Agilent Technologies) operating at 500 MHz for ^{1}H and 100 MHz for ^{13}C, respectively. Compounds were measured in $CDCl_3$ and the spectra referenced against residual non-deuterated solvents. HRESIMS were measured on a Agilent 6520 Time of Flight (TOF) MS instrument while GC-MS were recorded on a Hewlett Packard 6850 gas chromatograph coupled to a 5973 mass selective detector (Agilent Technologies). The fused silica capillary column was a DB-5MS column (Agilent Technologies). Electron impact (70 eV) mass spectra were recorded from *m/z* 50 to 550. The resulting data were elaborated using MSD ChemStation software (Agilent Technologies). Elemental analyses were obtained on a Perkin Elmer 240 B microanalyzer. Analytical data of the isolated compounds were in agreement within ± 0.4 % of the theoretical values. Column chromatography was carried out under TLC monitoring using silica gel (40-63 μm, Merck), and Sephadex LH-20 (25-100 μm, Pharmacia). For vacuum-liquid chromatography (VLC), silica gel (40-63 μm) (Merck) was used. TLC was performed on silica gel 60 F_{254} or RP-18 F_{254} (Merck). LiChrolut RP-18 (40-63 μm) 500 mg, 3mL (Merck) Solid Phase Extraction (SPE) cartridges were also used. Semi-preparative HPLC was conducted by means of a Varian 920 LH instrument fitted with an autosampler module with a 1000 μL loop. The peak purities were monitored using a dual-wavelength UV detector settled

at 254 and 366 nm. The columns were a 250 x 10 mm Spherisorb silica, particle size 5 μm (Waters) and a 250 x 10 mm Polaris C-18-A, particle size 5 μm (Varian).

Plant Material. The aerial parts of *B. fruticosum* were collected in July 2014 at Siniscola (Nu), Sardinia, Italy. The plant material was identified by Dr. Marco Leonti (University of Cagliari, Department of Biomedical Sciences). A voucher specimen (No. 0479) was deposited in the Herbarium of the Department of Life and Environmental Science, Drug Sciences Section, University of Cagliari.

Extraction and Isolation. Air-dried and powdered aerial parts of *B. fruticosum* (460 g) were ground and extracted with CH_2Cl_2 (5 L) by percolation at room temperature to give 23.5 g dried extract. An aliquot (20 g) of the CH_2Cl_2 extract was subjected to vacuum-liquid chromatography (VLC) (silica gel, 150 g, 40 - 63 μm) using a step gradient of *n*-hexane/EtOAc/MeOH (7.5:2.5:0 to 0:7.5:2.5, 500 mL each) to yield six main fractions (F1-F6). Fraction F3 (1.7 g) was separated by column chromatography over silica gel using CH_2Cl_2-EtOAc (9:1) as eluent giving eight subfractions (F3.1-F3.8). Fraction F3.1 (56 mg) was identified as compound **5** (11.1 mg). F3.2 (440 mg) was chromagraphed by CC over Sephadex LH-20 using MeOH as eluent to remove chlorophyll yielding three subfractions (F3.2.1-F3.2.3). Subfraction F3.2.3 (310 mg) was further purified by RP-18 SPE using acetonitrile as eluent to obtain compound **4** (270 mg). F3.3 (60 mg) was purified by CC over Sephadex LH-20 using MeOH as eluent to give an impure compound (12 mg) that was purified by RP-18 solid-phase extraction (SPE) using acetonitrile-H_2O (8.5:1.5) to give compound **8** (7.9 mg). Fraction F3.4 was chromatographed over Sephadex LH-20 (MeOH), followed by SPE (RP-18) using acetonitrile-H_2O (9:1) to give compound **10** (12.4 mg). Fraction F3.8 (120 mg) was purified using Sephadex LH-20 (MeOH) to produce compound **2**

(66.7 mg). F1 (1 g) was subjected to CC over silica gel using *n*-hexane-EtOAc (9:1) to give eight subfractions (F1.1-F1.8). F1.5 (70 mg) was purified by Sephadex LH (MeOH) yielding compound **7** (2.8 mg). F1.7 (250 mg) was purified over Sephadex LH-20 to remove chlorophyll to give a further fraction. This fraction (70 mg) was further subjected to CC over silica gel, using toluene-EtOAc (9:1) as eluent, to furnish compound **3** (16.9 mg) as a colorless oil. F4 (2.6 g) was subjected to CC over silica gel using CH_2Cl_2-MeOH (9.75:0.25) as eluent, to give eight subfractions (F4.1-F4.8). F4.2 was purified over Sephadex LH-20 (MeOH), followed by RP-HPLC, using acetonitrile-H2O (6:4, flow 2.5 mL/min) as eluent to provide compound **9** (2.3 mg, t_R 6.3 min). F4.8 was purified by CC over silica gel using n-hexane-EtOAc (6:4) as eluent to give compound **1** (110 mg). F2 (1g) was subjected to CC over silica gel, eluted with *n*-hexane-EtOAc (8:2) to give eight subfractions (F2.1-F2.8). F2.6 was purified by Sephadex LH-20, using MeOH as eluent, giving an impure compound that was further chromatographed by RP- HPLC using CH_2Cl_2 : EtOAc (9.75: 0.25, flow 2.5 ml/min) as eluent to give compound **6** (1.7 mg, t_R 6.5 min).

Fruticotriol (1): colorless oil; $[\alpha]^{25}_D$ -20.0 (*c* 0.09, CH_2Cl_2); ^1H ($CDCl_3$, 500 MHz) and ^{13}C ($CDCl_3$, 100 MHz) NMR, see Table 1; HRTOFESIMS *m/z* 289.1802 $[M - H]^+$ (calcd for $C_{18}H_{26}O_3$, 290.1803).

(-)-Eucamalol (10): colorless oil; $[\alpha]^{25}_D$ -17.0 (*c* 0.07, CH_2Cl_2); ^1H ($CDCl_3$, 500 MHz) and ^{13}C ($CDCl_3$, 100 MHz) NMR, see Table 1; EIMS *m/z* 168 $[M]^{+\cdot}$ (38), 139 $[M - CHO]^+$ (54), 125 $[M - C_3H_7]^+$ (77), 97 $[M - C_5H_{11}]^+$ (89), 69 $[C_5H_9]^+$ (100), 55 $[C_4H_7]^+$ (100); anal. C 71.27, H 9.48%, calcd for $C_{10}H_{16}O_2$, C 71.42, H 9.52%.

Homology Modeling. The structure of VP1-HRV39 was built with Swiss-model ProMod3 version 1.0.2.[26] The sequence of Coat protein VP1 of HRV39 was retrieved from the Uniprot

server. The retrieved sequence was fed into the BLAST search tool and the structure used as a template was 1AYM[28] that shares a 74% identity with our target structure. The multiple alignment of structures was performed with Clustal Omega.[27] The quality of the model was assessed by Swiss Model through the measure of qmean[30] and through the comparison with non-redundant PDB structure. In addition, the reliability of the model has been measured with ERRAT (UCLA-MBI),[30] a program for verifying the quality of the protein structures through the analysis of each single residue of the protein and PROCHECK.[31]

Ligand Preparation. The ligands were downloaded from the Protein Data Bank (PDB)[39] or built within Maestro GUI.[40] Their geometry was optimized. In particular, the compounds were subjected to a minimization protocol with MacroModel version 7.2,[41] considering MMFFs[42] as a force field and considering solvent effects by adopting the implicit solvation model Generalized Born/Surface Area (GB/SA) water.[43] The simulation was performed allowing 5000 steps Monte Carlo analysis with Polak-Ribier Conjugate Gradient (PRCG) method and a convergence criterion of 0.05 kcal/(mol Å).

Protein Preparation. Prior to performing docking experiments of known and isolated compounds, protein preparation was carried out starting from a protein structure model with PDB code 1AYM,[28] 1NCQ[35] and from the homology model of VP1-HRV39 using the protein preparation module in Maestro GUI.[40] All the water molecules were removed.

Molecular Docking and Post-docking. Docking experiments were performed using Quantum-mechanical polarized Docking (QMPL).[32,33] The Grid box was centred on the co-crystallized ligand and all parameters were set up as default. Cross-docking simulations were carried out in order to validate the protocol. Root-mean square deviation (RMSD) between the

crystallographic pose and the best binding pose of each compound ranked by Glide score were calculated. The validated protocol was then applied to compounds **4** and **5**. In order to take into consideration the induced fit phenomena, the best three poses of the two compounds were subjected to a post-docking procedure based on energy minimization using the molecular mechanics Generalized Born/Surface Area (MM-GBSA) method.[43] Figures were taken with Maestro GUI[40] and Pymol.[44]

Cells and Viruses. The cytotoxic and antiviral activities of the compounds was studied on both HeLa cells (Ohio strain) and Hep-2 cells grown in DMEM with 1% non-essential amino acids, 200 μg/mL streptomycin, 200 units/mL penicillin G and 10% fetal calf serum (Gibco Laboratories Inc.). Cell lines were kept at 37 °C in a humidified atmosphere with 5% CO_2. Rhinoviruses HRV14 (human rhinovirus species B) and HRV39 (human rhinovirus species A), were purchased from the American Type Culture Collection (ATCC). For all the above mentioned viruses, working stocks were prepared as cellular lysates using DMEM with 2% heat inactivated fetal calf serum.

Cytotoxic Activity. The cytotoxicity of the test compounds was evaluated by measuring the effect produced on cell morphology and cell growth in vitro. Cell monolayers were prepared in 24-well tissue culture plates and exposed to various concentrations of the compounds. Plates were checked by light microscopy after 24, 48 and 72 h. Cytotoxicity was scored as morphological alterations (e.g., rounding up, shrinking, detachment). The viability of the cells was determined by a tetrazolium-based colorimetric method using 3-(4,5-dimethylthiazol-2-yl)-2,5-diphenyltetrazolium bro-mide (MTT), as previously described.[45,46] The 50% cytotoxic dose (CC_{50}) is the concentration of the compound that reduced the absorbance of the control sample by 50%.

Inhibition of Virus Multiplication. The rhinovirus inhibition assay was evaluated by a one-step viral infection of cell monolayers, followed by virus yield titration in an agar-plaque assay. HeLa cell monolayers were prepared in 24 multiwell plates and were infected by the rhinoviruses at a MOI of 1. Next, serial dilutions of the test compounds were added and after 24–36 h of incubation at 33 °C and 3% CO_2, when the cytopathic effect in the control cells was almost total, the monolayers were frozen and thawed and the viruses in the supernatant were titrated by the plaque assay method. The antiviral activity assay on the rhinoviruses was carried out in a multi-cycle, virus-cell-based cytopathic effect (CPE) reduction assay in HeLa cells.[47] Pleconaril was used as reference compound. The compound concentration required to inhibit the CPE by 50% is expressed as the 50% inhibitory concentration (EC_{50}), and calculated by dose–response curves and linear regression.

Time-of-drug Addition Assay. Time-of-drug addition studies were performed on cell monolayers grown in 24 well plates, as indicated by Lacroix et al.[47] The compounds were added to the cells from h -1 to h +6 after viral infection. The cells were incubated in a CO_2 atmosphere for 24–36 h, washed twice with HBSS, after which virus yield inhibition (%) was determined by virus-cell-based cytopathic effect (CPE) reduction assay in HeLa cells. Pirodavir (5 μg/mL) was used as positive control.

Supporting Information

The Supporting Information is available free of charge on the ACS Publications website at DOI: …

Additional information (PDF).

AUTHOR INFORMATION

Corresponding Author

*Tel.: + 39-706758979; Fax: + 39-706758553; E-mail author: cottiglf@unica.it.

Author Contributions

▽These authors contributed equally.

The authors declare no competing financial interest.

ACKNOWLEDGMENTS

We are grateful to Prof. Marco Leonti of the Department of Biomedical Sciences, University of Cagliari, for the identification of the plant species for this study. This work was supported by Fondazione Banco di Sardegna (CAR 2014).

REFERENCES

(1) Jacobs, E. S.; Lamson, D. M.; George, K. St.; Walsh, T. J. *Clin. Microbiol. Rev.* **2013**, *26*, 135-162.

(2) World Health Organization. Programmes: Chronic Obstructive Pulmonary Disease (COPD)**.** http://www.who.int/respiratory/copd/en/.

(3) Senior, K. *Lancet Infect. Dis*. **2002**, *2*, 264.

(4) National Institutes of Health, USA. Clinical Trials. https://clinicaltrials.gov/ct/gui/show/NCT00394914.

(5) Andries, K. *Discovery of Pirodavir, a Broad-Spectrum Inhibitor of Rhinoviruses*. In *The Search for Antiviral Drugs*; Adams, J.; Merluzzi, V. J. Eds.; Brikhauser: Boston, 1993; pp 179−209.

(6) Thibaut, H. J.; Lacroix, C.; De Palma, A. M.; Franco, D.; Decramer, M.; Neyts, J. *Rev. Med. Virol.* **2016**, *26*, 21-33.

(7) Rollinger, J. M.; Schmidtke, M.; *Med. Res. Rev*. **2010**, *31*, 42-92.

(8) Ashoura, M. L.; Wink, M. J. *Pharm. Pharmacol*. **2011**, *63*, 305-321.

(9) Gunther, R.T. *The Greek Herbal of Dioscorides*, Hafner Publishing Company: London, 1968; p 297.

(10) Bremner, P.; Tang, S.; Birkmayer, H.; Fiebich, B. L.; Muñoz, E.; Marquez,N.; Rivera, D.; Heinrich, M. *Planta Med*. **2004**, *70*, 914-918.

(11) Pistelli, L.; Bilia, A. R. Bertoli, A.; Morelli, I.; Marsili, A. *J. Nat. Prod*. **1995**, *58*, 112-116.

(12) Massanet, M. G.; Guerra, F. M.; Jorge, Z. D.; Casalvázquez, L. G. *Phytochemistry* **1997**, *44*, 173-174.

(13) Pistelli, L.; Bertoli, A.; Bilia, A. R.; Morelli I. *Phytochemistry* **1996**, *41*, 1579-1582.

(14) Sonar, V. P.; Corona, A.; Distinto, S.; Maccioni, E.; Meleddu, R.: Fois, B.; Floris, C.; Malpure, N.V.; Alcaro, S.; Tramontano, E.; Cottiglia, F. *Eur. J. Med. Chem*. **2017**, *130*, 248-260.

(15) Tomkinson, N.; Wenlock, M.; McCrae, C. *Bioorg. Med. Chem. Lett*. **2012**, *22*, 7494-7498.

(16) Watanabe, K.; Shono, Y.; Kakimizu, A.; Okada A.; Matsuo, N.; Satoh, A.; Nishimura, H. *J. Agric. Food Chem*. **1993**, *41*, 2164-2166.

(17) Satoh, A.; Utamura, H.; Nakade, T.; Nishimura, H. *Biosci. Biotechnol. Biochem*. **1995**, *59*, 1139-1141.

(18) Kawazu, K.; Noguchi, H.; Fujishita, K.; Iwasa, J.; Egawa, H. *Tetrahedron Lett*. **1973**, *33*, 3131-3132.

(19) Su, B.-N.; Takaishi, Y.; Duan, H.-Q.; Chen, B. *J. Nat. Prod*. **1999**, *62*, 1363-1366.

(20) Liu, K.; Lota, M. L.; Casanova, J.; Tomi, F. *Chem. Biodivers*. **2009**, *6*, 2244-2254.

(21) Zhu, M.; Song, Y.; Cao, Y. *Synthesis* **2007**, *6*, 853-856.

(22) Feliciano, A. S.; Medarde, M.; Lopez, J. L.; Del Corral, J. M. M.; Barrero, A. F. *J. Nat. Prod.* **1986**, *49***,** 677-679.

(23) Roche, M.; Lacroix, C.; Khoumeri, O.; Franco, D.; Neyts, J.; Terme, T.; Leyssen, P.; Vanelle, P. *Eur. J. Med. Chem*. **2014**, *76*, 445-59.

(24) Da Costa, L.; Roche, M.; Scheers, E.; Coluccia, A.; Neyts, J.; Terme, T.; Leyssen, P.; Silvestri, R.; Vanelle, P. *Eur. J. Med. Chem*. **2016**, *115*, 453-462.

(25) Rollinger, J. M.; Steindl, T. M.; Shuster, D.; Kirchmair, J.; Anrain, K.; Ellmerer, E. P.; Langer, T.; Stuppner, H.; Wutzler, P.; Schmidtke, M. *J. Med. Chem*. **2008**, *51*, 843-851.

(26) Arnold, K.; Bordoli, L.; Kopp, J.; Schwede, T. *Bioinformatics* **2006**, *22*, 195-201.

(27) Sievers, F.; Wilm, A.; Dineen, D.; Gibson, T. J.; Karplus, K.; Li, W.; Lopez, R.; McWilliam, H.; Remmert, M.; Söding, J.; Thompson, J. D.; Higgins, D. G. *Mol. Syst. Biol*. **2011**, *7*: 539.

(28) Hadfield, A. T.; Lee, W.; Zhao, R.; Oliveira, M. A.; Minor, I.; Rueckert, R. R.; Rossmann, M. G. *Structure* **1997**, *5*, 427-441.

(29) Kim, K. H.; Willingmann, P.; Gong, Z. X.; Kremer, M. J.; Chapman, M. S.; Minor, I.; Oliveira, M. A.; Rossmann, M. G.; Andries, K.; Diana, G. D.; Dutko, F. J.; McKinlay, M. A.; Pevear, D. C. *J. Mol. Biol*. **1993**, *230*, 206-227.

(30) Colovos, C.; Yeates, T. O. *Protein Sci*. **1993**, *2*, 1511-1519.

(31) Morris, A. L.; MacArthur, M. W.; Hutchinson, E. G.; Thornton, J. M. *Proteins* **1992**, *12*, 345-364.

(32) Cho, A. E.; Guallar, V.; Berne, B. J.; Friesner, R. *J. Comput. Chem*. **2005**, *26*, 915-931.

(33) Chung, J. Y.; Hah, J. M.; Cho, A. E. *J. Chem Inf. Model*. **2009**, *49*, 2382-2387.

(34) Kollman, P. A.; Massova, I.; Reyes, C.; Kuhn, B.; Huo, S.; Chong, L.; Lee, M.; Lee, T.; Duan, Y.; Wang, W. *Accounts Chem. Res*. **2000**, *33*, 889-897.

(35) Zhang, Y.; Simpson, A. A.; Ledford, R. M.; Bator, C. M.; Chakravarty, S.; Skochko, G. A.; Demenczuk, T. M.; Watanyar, A.; Pevear, D. C.; Rossmann, M. G. *J. Virol*. **2004**, *78*, 11061-11069.

(36) Halgren, T.A. *J. Chem Inf. Model*. **2009,** *49*, 377-389.

(37) Oka, K.; Saito, F.; Yasuhara, T.; Sugimoto, A. *Contact Dermatitis* **1999**, *40*, 209-213.

(38) Leonti, M.; Casu, L.; Raduner, S.; Cottiglia, F.; Floris, C.; Altmann, K. H.; Gertsch, J. *Biochem. Pharmacol*. **2010**, *79*, 1815-1826.

(39) Berman, H. M.; Westbrook, J.; Feng, Z.; Gilliland, G.; Bhat, T. N.; Weissig, H.; Shindyalov, I. N.; Bourne, P. E. *Nucleic Acids Res*. **2000**, *28*, 235-42.

(40) Schrödinger, LLC. Maestro (GUI), New York, 2016.

(41) Mohamadi, F.; Richards N. G.; Guida, W. C.; Liskamp, R.; Lipton, M.; Caufield, C.; Chang, G.; Hendrickson, T.; Still, W. C. *J. Comput. Chem*. **1990**, *11*, 440-467.

(42) Halgren, T. A. *J. Comput. Chem*. **1996,** *17*, 520-552.

(43) Still, W. C.; Tempczyk, A.; Hawley, R. C.; Hendrickson, T. *J. Am. Chem. Soc*. **1990,** *112*, 6127-6129.

(44) Schrödinger, LLC. PyMOL Molecular Graphics System, New York, 2014

(45) Norman, P. J.; Ager, A.L.; Bliss, R. A.; Canfield, C. J.; Kotecka, B. M.; K. Rieckmann, H.; Terpinski, J.; Jacobus, D. P. *J. Med. Chem*. **2001**, *44*, 3925-3931.

(46) Denizot, F.; Lang, R.; *J. Immunol. Methods* **1986**, *89*, 271-277.

(47) Lacroix, C.; Laconi, S.; Angius, F.; Coluccia, A.; Silvestri, R.; Pompei, R.; Neyts, J.; Leyssen, P. *Virol. J.* **2015,** *12*: 106.

SYNOPSIS GRAPHIC

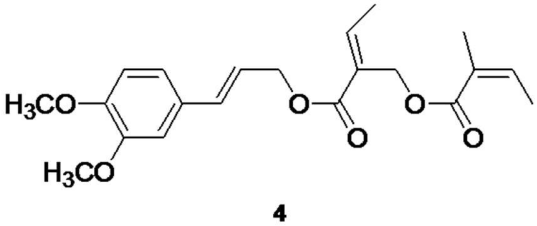

4